Journal of Environmental Statistics
August 2013, Volume 5, Issue 4. http://www.jenvstat.org

Statistical Climate-Change Scenarios

Jan R. Magnus
Vrije Universiteit Amsterdam

Bertrand Melenberg
Tilburg University

Chris Muris
Simon Fraser University

Martin Wild
ETH, Zürich

Abstract

We report on climate projections generated by a simple model of climate change. The model captures the effects of variations in surface solar radiation, using information over the period 1959–2002 available from observational records from the Global Energy Balance Archive (GEBA), as well as increases in greenhouse gases on surface temperature. The model performs well with respect to observational data, and is simple enough to admit a rigorous statistical analysis. This allows us to quantify the uncertainty associated with estimated parameter values using observational data only. Our method immediately leads to estimates with associated confidence intervals, which can be translated into confidence intervals for climate projections. In particular, we construct probabilistic climate projections using standard scenarios for carbon dioxide and sulphur dioxide emissions.

Keywords: global warming, dimming, aerosols, projections.

1. Introduction

Changes in the concentrations of greenhouse gases and aerosols are the two most important drivers of man-made climate change. Modeling the processes through which these two variables affect our climate is therefore an essential ingredient of any climate model. Using scenario analysis, these climate models are then used to provide policy makers with climate projections, conditional on hypothesized changes in greenhouse gas and aerosol emissions.

Uncertainty plays an important role in modeling and projecting climatic change; see, for example, Andreae et al. (2005), Stainforth et al. (2005), and Roe and Baker (2007). Given a climate model, uncertainty about the parameter values leads to uncertainty in the implied climate projections. While consensus exists on the values of some parameters, there is much

uncertainty on many key parameter values, for example the value of climate sensitivity and the aerosol effect; see, for instance, Schwartz et al. (2010) and Knutti and Plattner (2012).

Our aim is to formulate a climate model, which is simple enough to allow a rigorous statistical analysis, but not so simple that it ignores key climate ingredients. The simplicity is essential for our purpose, because it implies that we can estimate the parameters of the climate model with conventional statistical methods. This has the advantage that we can quantify the uncertainty associated with the estimated parameter values. In other words, we let observational data tell us how confident we can be about the parameter values for our model, and how well the model fits the data. We then translate this uncertainty into confidence intervals for projections of future climate under various scenarios.

The starting point is a model recently proposed in Magnus et al. (2011) who attempted to disentangle the counteracting effects on surface temperature of the observed reductions of surface solar radiation and of increases of greenhouse gases. The parameters of this model are estimated using observational data over the period 1959–2002 obtained from the Global Energy Balance Archive (GEBA), and surface temperature and CO2 concentration data. In order to conduct scenario analysis, we augment this model in two directions. First, we provide carbon and aerosol models, linking emissions to concentrations. Second, we develop a model that allows us to distinguish between model error and measurement error. We then estimate the parameters in these models, quantify the uncertainty associated with the estimates, and apply our model to typical climate scenarios.

The simplicity of the model allows us to quantify the uncertainty associated with estimated parameter values using observational data only. As a consequence, our method immediately leads to estimates with associated confidence intervals, which are translated into confidence intervals for climate projections. In this way, our statistical approach differs from the probabilistic approach employed by the IPCC; see Meehl et al. (2007). The latter approach makes use of models, based on physical principles, that are more advanced and closer to reality. Such advanced models are typically characterized by many parameters, and as such, too complex to be estimated directly, solely on the basis of observational data. Instead, they have to be validated using indirect methods using implied relationships, for instance, by confronting model-based values of the climate sensitivity with empirical estimates of this quantity; see, for instance, Knutti and Hegerl (2008) and references therein. Probabilistic climate projections using advanced and complex models can then be obtained by varying the parameters over such indirectly validated values. Our observationally-based approach can be seen as a *direct* way to validate this procedure: our relationships, estimated (in-sample) using observational data, are directly 'extrapolated' into (out-of-sample) climate projections, given typical climate scenarios. Finding substantial differences between the two approaches would require at least that this difference is not caused by the indirect validation. However, our findings do not invalidate the IPCC outcomes.

The remainder of this paper is organized as follows. The energy balance is discussed in Section 2. In Section 3, we introduce uncertainty in the energy balance equation, leading to a statistical model, and describe the data used to estimate this statistical model. In Section 4 we decompose this uncertainty into process risk and measurement error. In Section 5 we provide a simple link between emissions and concentrations. This completes the model. Section 6 briefly describes the three scenarios that we consider. Section 7 contains the results of our scenario and validation analysis, and Section 8 concludes. A data appendix contains additional information about the emission data used for estimating the link between emissions

and concentrations proposed in Section 5.

2. The energy balance

Our starting point is the energy balance equation,

$$c \cdot \frac{d\text{TEMP}_t}{dt} = \text{EB}_t, \tag{1}$$

where TEMP_t denotes the surface temperature at time t (measured in degrees Celsius), EB_t is the energy balance, c the heat capacity, and $d\text{TEMP}_t/dt$ the derivative of TEMP_t with respect to time t. Decomposing the energy balance as in Wild et al. (2004), gives

$$\text{EB}_t = \text{SW}_t^{\text{abs}} + \text{LW}_t^{\text{down}} + \text{LW}_t^{\text{up}} + \text{SH}_t + \text{LH}_t + \text{GH}_t + \text{M}_t, \tag{2}$$

where SW^{abs} is the absorbed shortwave radiative flux, LW^{down} and LW^{up} are the downward and upward longwave radiative fluxes, SH and LH are the sensible and latent heat fluxes, GH is the ground heat flux, and M is the energy flux used for melt.

Wild et al. (2004) analyzed the change in energy fluxes over the period 1960–1990. For their purpose it sufficed to consider the stationary perturbation surface temperature, so that $\Delta\text{EB}_t = 0$, where Δ denotes a change per unit of time: $\Delta x_{t+1} = x_{t+1} - x_t$. In contrast, we implement (1) using annual data from observational sites (which include measures of surface solar radiation along with conventional synoptic weather information). We describe these observational data in detail in the next section. To transform the energy balance equation to annual changes in temperature we integrate (1) over a one-year period,

$$c \int_t^{t+1} \frac{d\text{TEMP}_\tau}{d\tau}\, d\tau = \int_t^{t+1} \text{EB}_\tau\, d\tau, \tag{3}$$

leading to the approximation

$$c\,(\text{TEMP}_{t+1} - \text{TEMP}_t) \approx \text{EB}_t. \tag{4}$$

The approximation will be more accurate when we measure the energy balance EB_t as a one-year average, because seasonal effects are then balanced out, and this is what we shall do in our empirical analysis. Assuming equality in (4), we write the equation in differences (over one-year periods),

$$c\Delta\text{TEMP}_{t+1} = \Delta\text{EB}_t + c\Delta\text{TEMP}_t. \tag{5}$$

We next specify the energy balance term ΔEB_t. Given (2) and assuming that changes in the ground heat flux GH_t and the energy flux used for melt M_t are negligible (Wild et al., 2004, Table 1; Wild et al., 2008, Table 1), we obtain

$$\Delta\text{EB}_t = \Delta\text{NSR}_t + \Delta\text{SH}_t + \Delta\text{LH}_t,$$

where NSR denotes the net surface radiation

$$\text{NSR} = \text{SW}^{\text{abs}} + \text{LW}^{\text{down}} + \text{LW}^{\text{up}}.$$

Following Magnus et al. (2011) we parameterize the terms in the net surface radiation equation as

$$\begin{aligned} \mathrm{SW}_t^{\mathrm{abs}} &= (1-\alpha_1)\mathrm{RAD}_t, \\ \mathrm{LW}_t^{\mathrm{down}} &= \alpha_2 + \alpha_3 \log(\mathrm{CO2}_t), \\ \mathrm{LW}_t^{\mathrm{up}} &= \alpha_4 + \alpha_5 \mathrm{TEMP}_t, \end{aligned}$$

and this leads to

$$\Delta\mathrm{NSR}_t = (1-\alpha_1)\Delta\mathrm{RAD}_t + \alpha_3 \Delta \log(\mathrm{CO2}_t) + \alpha_5 \Delta\mathrm{TEMP}_t. \tag{6}$$

In these equations, RAD_t stands for the solar surface radiation, that is the solar radiation reaching the Earth's surface (measured in Watts per meter squared), and $\mathrm{CO2}_t$ stands for the carbon dioxide concentration (measured in parts per million by volume). To close the model we need to parameterize the latent and sensible heat fluxes. We shall assume that changes in these fluxes are proportional to changes in the net surface radiation, that is,

$$\Delta\mathrm{SH}_t = \alpha_6 \Delta\mathrm{NSR}_t, \qquad \Delta\mathrm{LH}_t = \alpha_7 \Delta\mathrm{NSR}_t. \tag{7}$$

Then, substituting (6) and (7) into (5), we find

$$\Delta\mathrm{TEMP}_{t+1} = \beta_1 \Delta\mathrm{TEMP}_t + \beta_2 \Delta\mathrm{RAD}_t + \beta_3 \Delta \log(\mathrm{CO2}_t), \tag{8}$$

where the β's are linear combinations of the α's.

3. The statistical model

For each site in our observational data set, we apply this model for every year for which data is available. Because of neglected terms, approximation errors in the parametrization, and possible measurement errors, we allow for stochastic error terms, $\Delta u_{i,t+1}$, for each observational site for each time period, and a time-specific temperature change $\Delta\lambda_{t+1}$ that is common to all weather stations:

$$\Delta\mathrm{TEMP}_{i,t+1} = \beta_1 \Delta\mathrm{TEMP}_{i,t} + \beta_2 \Delta\mathrm{RAD}_{i,t} + \Delta\lambda_{t+1} + \Delta u_{i,t+1}. \tag{9}$$

The time-specific temperature change depends on global average temperature, global average surface solar radiation, carbon dioxide concentration, and an additive stochastic error term:

$$\Delta\lambda_{t+1} = \gamma_1 \Delta\overline{\mathrm{TEMP}}_t + \gamma_2 \Delta\overline{\mathrm{RAD}}_t + \gamma_3 \Delta \log(\mathrm{CO2}_t) + \eta_{t+1}, \tag{10}$$

where global averages are denoted by a horizontal line over the variable. This specification is the same as Equations (10) and (11) in Magnus et al. (2011), though obtained via a different route.

To estimate Equations (9) and (10), we collected monthly observations on three variables:

- temperature (TEMP), the average temperature in degrees Celsius (°C) at the surface (the near-surface temperature), as expressed as anomalies from a base period (1960–1990). *Source:* Climatic Research Unit (CRU TS 2.1) at the University of East Anglia in the UK (Mitchell and Jones, 2005), see http://www.cru.uea.ac.uk;

- surface solar radiation (RAD), the amount of sunlight ('global solar irradiance') reaching the Earth's surface, measured in Watts per meter squared (Wm^{-2}). *Source:* Global Energy Balance Archive (GEBA) (Gilgen and Ohmura, 1999);
- carbon dioxide concentration (CO2), measured in parts per million by volume (ppmv). *Source:* Mauna Loa Observatory (MLO) in Hawaii, see http://www.mlo.noaa.gov/

Data from the three sources are linked through their locations. The radiation data are incomplete. We circumvent a potential sample selection problem by considering temperature changes rather than temperature levels. We use annual data rather than monthly data to avoid problems of seasonal adjustment. This provides us with $N = 1337$ observational sites over a period of $T = 44$ years (1959–2002).

The parameters are estimated using the generalized method of moments (GMM) approach using appropriate moment restrictions, following Arellano and Bond (1991), Blundell and Bond (1998), and Magnus et al. (2011). The resulting parameter estimates and their standard errors are

$$\begin{aligned}\Delta\mathrm{TEMP}_{i,t+1} = {} & 0.9063\,\Delta\mathrm{TEMP}_{i,t} + 0.0087\,\Delta\mathrm{RAD}_{i,t} + \Delta\lambda_{t+1} + \Delta u_{i,t+1} \\ & (0.0046) \qquad\quad (0.0008)\end{aligned} \tag{11}$$

and

$$\begin{aligned}\Delta\lambda_{t+1} = {} & -0.8235\,\Delta\overline{\mathrm{TEMP}}_t + 0.0614\,\Delta\overline{\mathrm{RAD}}_t + 10.6955\,\Delta\log(\mathrm{CO2}_t) + \eta_{t+1}. \\ & (0.1839) \qquad\quad (0.0219) \qquad\quad (2.3958)\end{aligned} \tag{12}$$

Averaging over (11) and combining with (12) then leads to

$$\begin{aligned}\Delta\overline{\mathrm{TEMP}}_{t+1} = {} & 0.0828\,\Delta\overline{\mathrm{TEMP}}_t + 0.0701\,\Delta\overline{\mathrm{RAD}}_t + 10.6955\,\Delta\log(\mathrm{CO2}_t) + \eta_{t+1} \\ & (0.1839) \qquad\quad (0.0219) \qquad\quad (2.3958)\end{aligned} \tag{13}$$

where we have assumed that $\Delta\bar{u}_{t+1} = 0$. The estimates in (11) are much more accurate than those in (12). There is not much loss, therefore, if we calculate the standard errors in (13) based on the standard errors in (12) alone.

In the sequel we shall write (13) briefly as

$$\Delta\overline{\mathrm{TEMP}}_{t+1} = \mu_t + \eta_{t+1}, \tag{14}$$

with μ_t representing the 'systematic' part, depending on lagged temperature, surface solar radiation, and carbon dioxide concentration, and η_{t+1} the so-called 'idiosyncratic' part of the average temperature change, that is the change in temperature not captured by the systematic part.

4. Specification of η_{t+1}

We wish to apply (14) to forecasting and scenario analysis. Since the uncertainty in our model is driven by observational data, such a scenario analysis will give a realistic view of the degree of uncertainty about future climate change. There are, however, two problems that need to

be resolved before we can attempt this analysis. First, we need to specify how the errors η_{t+1} are generated. Second, inputs to the model are carbon dioxide concentration CO2 and surface solar radiation RAD, while the scenarios are in terms of emissions of CO2 and SO2, so we need a link between these emissions and the inputs to the model. We deal with each issue in turn. The current section discusses the specification of the errors η_{t+1}, and the next section proposes simple models which transform carbon dioxide emissions to concentrations and sulphur dioxide emissions to surface solar radiation.

The idiosyncratic error term η_{t+1} in (14) consists of idiosyncratic process risk (representing natural variations in the average temperature change not captured by the systematic part μ_t) and measurement error. We shall identify this measurement error, so that it does not enter into our climate projections. To do so, we compare a time series based on our data set (the CRU TS 2.1 series) to the global means of the CRUTEM3v data set (see Brohan et al., 2006). These data sets overlap in terms of the basic temperature series, but are different in their coverage and how they are constructed. The coverage of our data set is restricted to the 1337 observational sites in our data set, while the CRUTEM3v uses data on all observational sites available for the period under consideration. To arrive at a global mean temperature, we use a simple averaging method, while a more sophisticated algorithm was used for CRUTEM3v. In terms of temperature differences there is no selection bias (see Magnus et al., 2011), but there might be a difference in the measurement error of these two temperature series. We therefore propose the following set-up, where the superscript C refers to the CRUTEM3v temperature series:

$$\Delta\overline{\mathrm{TEMP}}_{t+1} = \mu_t + \eta_{t+1} = \mu_t + \eta^*_{t+1} + \epsilon_{t+1},$$
$$\Delta\overline{\mathrm{TEMP}}^C_{t+1} = \mu_t + \eta^C_{t+1} = \mu_t + \eta^*_{t+1} + \epsilon^C_{t+1}.$$

Here, η^*_{t+1} denotes the idiosyncratic process risk, and ϵ_{t+1} and ϵ^C_{t+1} represent the measurement error in the temperature series used in the estimation procedure and the CRUTEM3v temperature series, respectively. The systematic part μ_t and the idiosyncratic process risk η^*_{t+1} are the same for both temperature series, while each temperature series is assumed to have its own measurement error.

Our aim is to retrieve the idiosyncratic process risk η^*_{t+1}. We cannot, however, retrieve three error terms (η^*_{t+1}, ϵ_{t+1}, ϵ^C_{t+1}) from two observed temperature series. Therefore we propose, in addition, that the two measurement errors are proportional, that is,

$$\epsilon^C_{t+1} = f \times \epsilon_{t+1},$$

for some fraction f, constant over time. Given f, we can identify ('solve') η^*_{t+1}.

We choose f such that the sample correlation between the idiosyncratic process risk and the measurement error vanishes in both series. The condition $\mathsf{COV}(\eta^*_{t+1}, \epsilon_{t+1}) = 0$ leads to the estimate $\widehat{f} = 0.0826$, so that

$$\eta^*_{t+1} = \frac{\eta^C_{t+1} - \widehat{f}\eta_{t+1}}{1 - \widehat{f}} = 1.09\,\eta^C_{t+1} - 0.09\,\eta_{t+1}.$$

The low value of $\widehat{f}$ shows that the measurement error in the CRUTEM3v temperature data series is smaller than in the data that we use (the CRU TS 2.1 series). This is as expected, as our data consist of just one of the series that are used for computing the CRUTEM3v series.

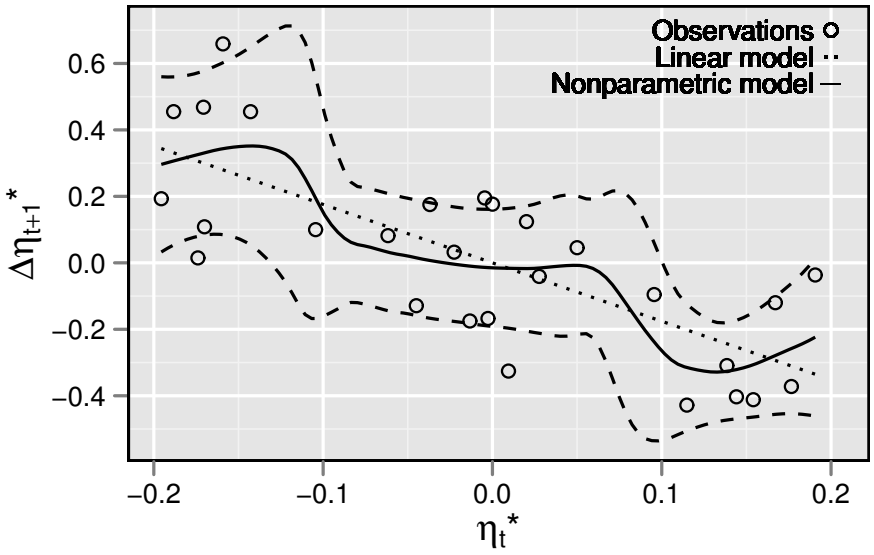

Figure 1: Justifiability of the Ornstein-Uhlenbeck process

Given this estimated value of f, the total estimated variance of η_{t+1} (0.1589) is equal to the sum of the estimated variance of η_t^* (0.0505) and the estimated variance of ϵ_{t+1} (0.1084).

Now that we have data on the idiosyncratic process risk η_{t+1}^*, we specify the underlying process as follows. Following Majda at al. (2001), Vallis et al. (2004), and Padilla et al. (2011), we model η_{t+1}^* as an Ornstein-Uhlenbeck type process:

$$\Delta\eta_{t+1}^* = -\alpha\eta_t^* + \zeta_{t+1}, \qquad \zeta_{t+1} \overset{iid}{\sim} \left(0, \sigma_\zeta^2\right). \tag{15}$$

The dotted line in Figure 1 shows the regression for $\widehat{\alpha} = -1.7582$, restricted to the range $\eta_t^* \in [-0.2, +0.2]$. The figure also plots the nonparametric estimate of g in

$$\Delta\eta_{t+1}^* = g(\eta_t^*) + \omega_{t+1}, \qquad E\left(\omega_{t+1}|\eta_t^*\right) = 0,$$

together with the corresponding 95% uniform confidence band, where we apply Härdle and Linton (1994, eq. (29)), using the quartic kernel and bandwidth chosen according to Silverman's rule of thumb with some undersmoothing. (Without this undersmoothing, the nonparametric graph would be close to linear.) The nonparametric regression provides empirical evidence in support of modeling the temperature error by means of an Ornstein-Uhlenbeck type process. The resulting estimated variance of ζ_{t+1} is $\widehat{\sigma}_\zeta^2 = 0.0347$. The subsequent results are based on this model for the error process.

5. Emissions and concentrations

Climate scenarios are usually specified in terms of emissions, not in terms of concentrations. For example, a scenario may prescribe a specific increase in carbon dioxide emissions or a decrease in sulphur dioxide emissions. Our energy balance model (9)–(10) is formulated in

terms of CO2 concentration and surface solar radiation. Hence, we need auxiliary models that transform carbon dioxide emissions into carbon dioxide concentrations, and sulphur dioxide emissions into levels of surface solar radiation. Although there are also, for example, SRES CO2 concentration scenarios, we prefer to use our own transformations from emissions to concentrations, in order to be able to quantify the uncertainties arising from the use of observational data.

The auxiliary models presented in this section follow the general philosophy of the paper in that they are simple models analyzed in a statistically rigorous way. They are sufficiently simple that they can be estimated using conventional statistical techniques, so that we can incorporate the uncertainty in the estimates of the model parameters in our climate projections. This allows us to use the augmented model to convert scenario data — CO2 and SO2 emissions — into probabilistic climate projections that take the uncertainty into account at every step of the modeling process. The emission data used for estimation are described in the data appendix.

We estimate a linear regression between the change in carbon dioxide concentrations (ΔCO2) and CO2 emissions (CE):

$$\begin{aligned} \Delta \mathrm{CO2}_t = {} & 0.0993 + 0.2436\,\mathrm{CE}_t + v_t. \\ & (0.0404)\ \ (0.0521) \end{aligned} \tag{16}$$

In addition, we estimate a linear regression linking global average surface solar radiation ($\overline{\mathrm{RAD}}$) to aggregate SO2 emission (SE).

$$\begin{aligned} \overline{\mathrm{RAD}}_t = {} & 59.1272 - 15.4063\,\log(\mathrm{SE}_t) - 0.2872\,(t-1958) + w_t \\ & (7.4184)\quad (1.7954)\qquad\quad (0.0169). \end{aligned} \tag{17}$$

Equation (17) does not aim to provide a structural model for average surface solar radiation in terms of aggregate SO2 emission. The equation simply represents an *empirical* link, based on past data, for the purpose of transforming SO2 emission data into average surface solar radiation data. We shall interpret the time trend as reflecting growth, which, measured by world GDP in logarithmic terms, is very close to linear as a function of time. Growth likely results in emissions not captured by SO2 emissions. These omitted emissions might affect the surface solar radiation directly, like SO2 emissions, or indirectly, such as greenhouse gases, including CO2, that influence the surface solar radiation via increasing cloud thickness, as suggested by Tselioudis and Rossow (1994). For a review of the literature on the relationship between aerosols (such as sulphur dioxide) and surface solar radiation, see Wild (2009). The data used to estimate these models are described in the data appendix.

The energy balance model (9)–(10) resulting in (13), together with the error specification (15) and the two auxiliary equations (16) and (17) constitute our augmented climate model. Its performance is illustrated in Figures 2 and 3.

The left panel of Figure 2 describes the in-sample fit of the carbon model (16), while the right panel of Figure 2 presents the aerosol-surface solar radiation model (17), with the level of average surface solar radiation measured in Wm^{-2} in deviation of the average level of surface solar radiation in 1959. The small circles are the actual observations, the solid curves the in-sample forecasts (starting at the beginning of the sample), and the dashed curves are uncertainty bands. We include both parameter and process uncertainty, using 5000 simulations. In each simulation, parameters are drawn from joint asymptotic normal distributions,

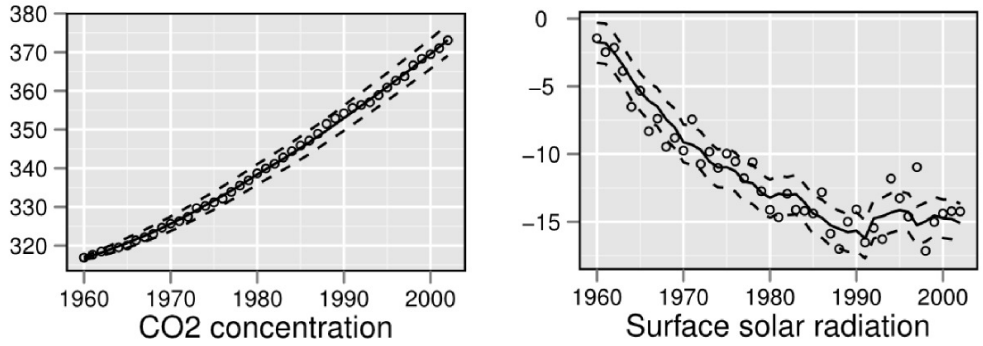

Figure 2: In-sample predictions for CO2 concentration, measured in parts per million by volume (ppmv) (left panel), and surface solar radiation, measured in Watts per meter squared (Wm^{-2}), in deviation of the average level of surface solar radiation in 1959 (right panel).

representing parameter uncertainty, while the error terms are drawn from the corresponding sample error distributions, representing process uncertainty. The dashed curves depict the range of 'likely outcomes', based on these 5000 simulations. (In contrast to statistical practice, where 95% bands are typically used, the IPCC defines an outcome as 'likely' when it falls within the 67% confidence band.) We conclude that our models describe the data with sufficient accuracy.

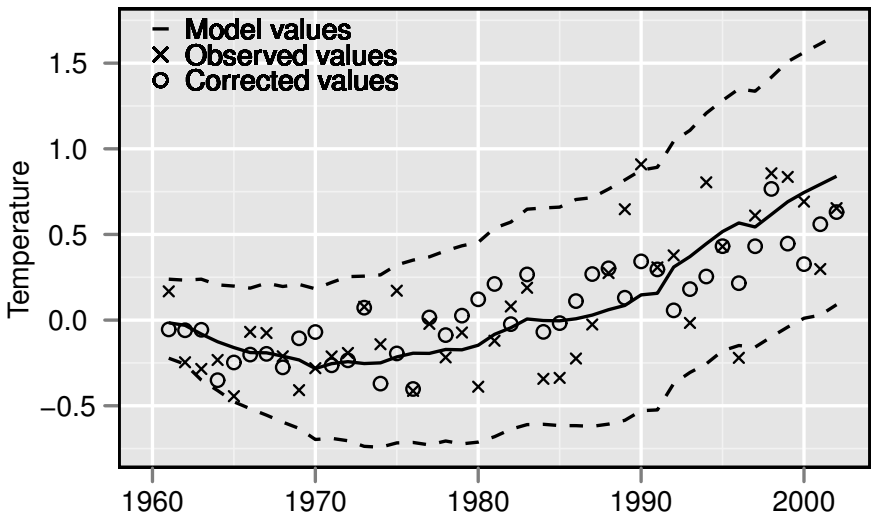

Figure 3: In-sample predictions for temperature, measured in degrees Celsius (°C), with the temperature in 2002 set equal to 0.8 °C.

Further evidence is provided by Figure 3, which shows that the trends in the temperature series are well captured by our simple model. The points denoted × are the observed values and the small circles are the values corrected for measurement error. The solid line gives the

in-sample fit and the dashed lines are 67% confidence bands. All curves are normalized so that their in-sample mean coincides with the mean of the temperature series. The temperature is measured with the pre-industrialization temperature set equal to 0 °C. On average, the corrected measurements are closer to the model values, and both the observed and corrected values are (broadly) within the 67% confidence band.

6. Scenarios

We now have an integrated model of climatic change, estimated its parameters, and verified that the model provides a satisfactory description of the temperature series. Before we can analyze scenarios in the next section, we need to decide which scenarios we wish to consider.

We shall consider three scenarios. First, a baseline model, denoted '00', in which carbon dioxide and sulphur dioxide emissions are kept constant at their end-of-sample values (2002). The other two scenarios are publicly available IPCC scenarios (SRES) to facilitate comparison between our projections and those of other modeling groups. The SRES scenarios that we analyze are known as 'A1T' and 'A1FI'.

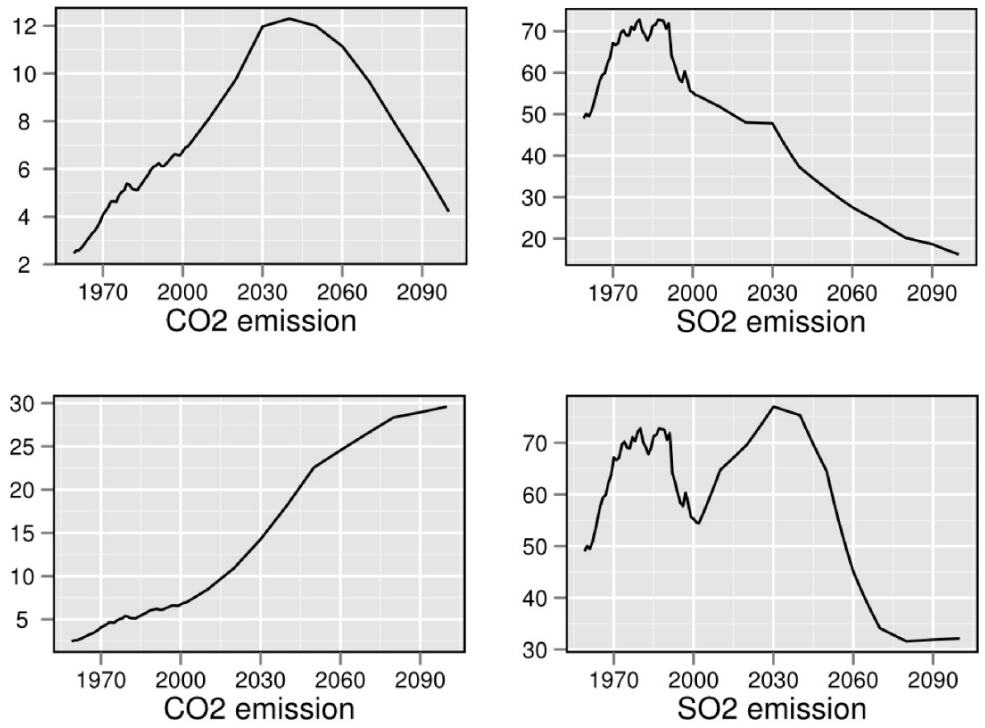

Figure 4: Emissions scenarios (top: A1T, bottom: A1FI) for CO2, measured in millions of metric tons of carbon (left panel), and SO2, measured in metric tons of sulfur (right panel). [Caption goes here]

Both scenarios are part of the A1 storyline, which postulates rapid and continuing economic growth, a global population that reaches around 9 billion in 2050 and then gradually declines, and a rapid introduction of new and more efficient technologies. The main difference between

A1T and A1FI is that A1T emphasizes the use of alternatives to fossil energy sources, while A1FI describes a world that intensively uses fossil energy sources. For more information about the IPCC/SRES scenarios, see Nakicenovic and Swart (2000).

The SRES SO2 emission scenarios do not match the realization in the period 1990–2000. A reversal of the trend after 1990 was already reported by Stern (2006). In particular, the economic downturn in the former USSR and Eastern Europe after 1989 resulted in a substantial reduction in SO2 emissions, and the SRES scenarios do not take this reduction into account. If we were to use the post-2000 levels of the SRES scenarios without adaptation, then a serious jump-off bias would result, compared to the actual in-sample values. For this reason, we create adapted SRES scenarios which do not suffer from jump-off bias. We follow the same strategy for the CO2 emission scenarios, although here the jump-off bias is much less serious.

To illustrate the resulting emission scenarios, Figure 4 presents a time- series plot of the carbon dioxide and sulphur dioxide emissions corresponding to scenarios A1T and A1FI. Our resulting scenarios are similar to the original SRES scenarios, but adapted to the actual levels. The emissions are quite different in the two scenarios. The carbon dioxide emission reaches a maximum around 2040 in scenario A1T, but continues to increase in scenario A1FI during the whole period, be it with some slowdown in growth after 2050. The sulphur dioxide emission continues to decrease in scenario A1T after the drop in the 1990s, but in scenario A1FI the emission first increases again until 2040, and then decreases to become more or less stable from 2080 onwards.

To complete our scenarios, we also have to extrapolate the linear time trend in the empirical surface solar radiation equation (17). Our interpretation of this time trend is economic growth as measured by world real GDP. According to the SRES A1 scenarios, world real GDP will continue to increase more or less exponentially, so that its logarithm will increase more or less linearly as a function of time. Thus we extrapolate the linear time trend in the empirical surface solar radiation equation linearly by extending the linear in-sample trend.

7. Projections

We now present the results of our scenario analysis. Figure 5 projects the changes in carbon dioxide concentration and surface solar radiation for scenarios A1T and A1FI. More precisely, for scenario A1T, the top panel of Figure 5 presents the projections of the estimated carbon and aerosol-surface solar radiation models (16) and (17), resulting from the emissions illustrated in the top of Figure 4, together with the time trend in the empirical surface solar radiation equation, extrapolated linearly. The bottom panel of Figure 5 provides the projections for scenario A1FI, based on the bottom panel of Figure 4. The dashed lines correspond to 67%-confidence intervals, taking into account both parameter and process uncertainty.

The uncertainty is more pronounced as we move forward in time, exactly as one would expect. The conversion from CO2 emissions to CO2 concentration is slow, which is why the resulting graphs are smoother than their inputs. The decrease in CO2 emission after 2040 in the A1T scenario results in a slowdown of CO2 concentration growth. In the A1FI scenario the growth in CO2 concentration speeds up over time. The surface solar radiation patterns follow the SO2 patterns closely, but with a downward trend over time due to the extrapolated linear time trend, reflecting continuous economic growth as measured by GDP (see also section 5,

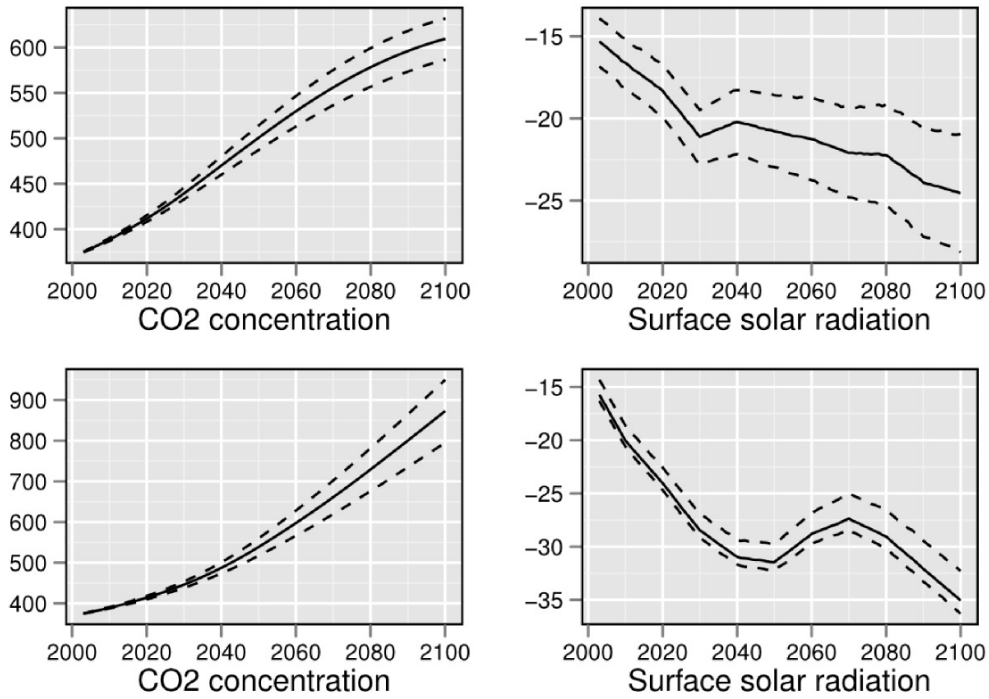

Figure 5: Projections (top: A1T, bottom: A1FI): CO2 concentration, measured in parts per million by volume (ppmv) (left panel), and surface solar radiation, measured in Watts per meter squared (Wm^{-2}), in deviation of the average level of surface solar radiation in 1959 (right panel).

where we link economic growth to emissions not captured by SO2 emissions).

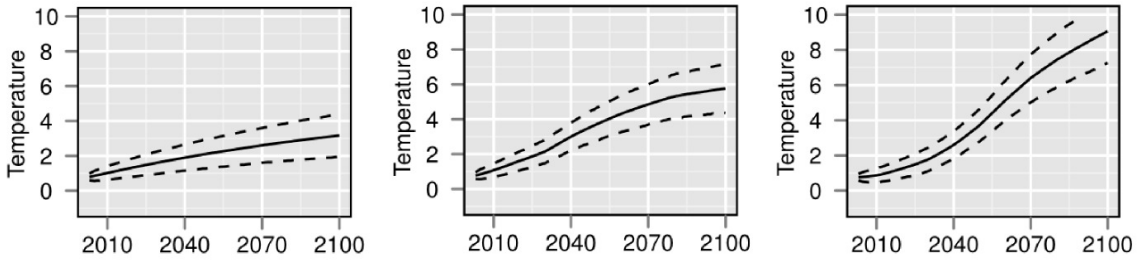

Figure 6: Temperature projections: 00 (left), A1T (middle), and A1FI (right). Temperature is measured in degrees Celsius (°C), with the temperature in 2002 set equal to 0.8 °C.

Figure 6 presents our probabilistic temperature projections for the three scenarios 00, A1T, and A1FI. The solid curve shows the temperature forecast (mean over 5000 simulations), while the dashed curves represent the range of likely outcomes (the 67%-confidence interval), accounting for both parameter and process uncertainty. The temperature is measured with the pre-industrialization temperature set to zero.

Without any change in the inputs (scenario 00, left panel), the mean temperature in 2100 (averaged over all scenarios) lies around 3.1 °C, and the likely range is (1.9°C, 4.4°C). Keeping the emissions at their end-of-sample values results in a continuing increase of CO2 concentration, which has a positive effect on temperature, while a constant SO2 emission level does not result in an extra reduction (apart from the time trend) in average surface solar radiation according to our empirical relation (17), and thus no extra negative effect on temperature. The net effect is an increase in temperature.

In scenario A1T (middle) we project a temperature increase in 2100 of about 5.7°C, with a likely range of (4.3°C, 7.0°C). CO2 emissions are higher than in scenario 00, resulting in higher CO2 concentration and higher temperature. At the same time, the decreasing SO2 emission levels result in only moderate changes in surface solar radiation, corresponding to only moderate changes in temperature. The net effect is a stronger temperature increase than in scenario 00.

The results for scenario A1FI (right panel) are based on CO2 and SO2 emissions that are higher than in scenario A1T. Higher CO2 emissions positively affect temperature, and this detoriates the cooling effect of the increase in SO2 emissions. The resulting temperature increase in 2100 is higher than for A1T, around 8.9°C, with likely range (7.2°C, 10.7°C).

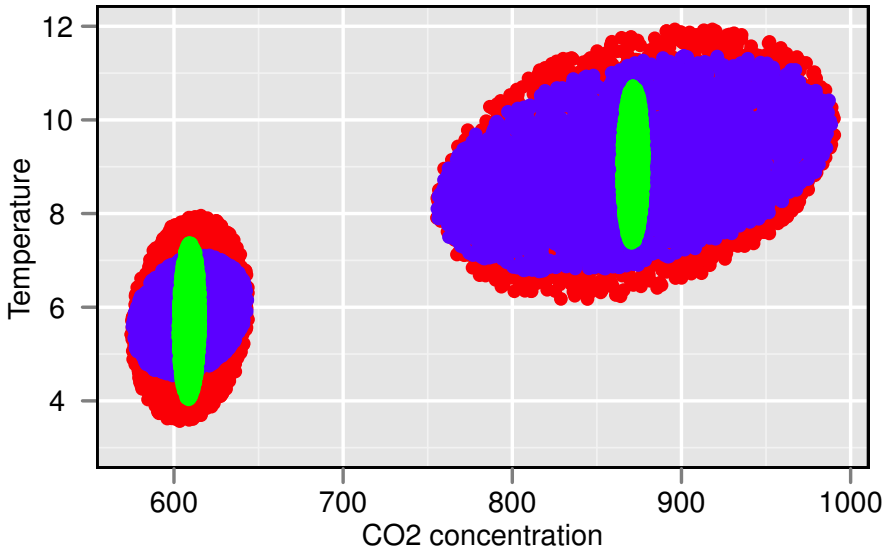

Figure 7: Projections of likely temperature and CO2 concentration combinations (left: A1T, right: A1FI). Temperature is measured in degrees Celsius (°C), with the temperature in 2002 set equal to 0.8 °C. CO2 concentration is measured in parts per million by volume (ppmv).

In Figure 7 we complement the projections of Figure 6 by presenting the joint 67%-confidence set for CO2 concentration and temperature. We distinguish between process risk (green), parameter risk (blue), and combined risk (red). The lower-left confidence set corresponds to scenario A1T, and the upper-right confidence set to scenario A1FI. The process risk (green areas) is more or less of the same size in both cases. But the higher input levels in scenario A1FI generate substantially more parameter risk than in scenario A1T, resulting in a much

larger 67%-confidence set. This is particularly so in the CO2 concentration dimension.

Compared to Solomon et al. (2007, Chapter 10) we find similar levels in CO2 concentrations, but higher temperature increases in both scenarios A1T and A1FI. Focusing on temperature, we do find similar lengths of the likely ranges. For scenario A1T, Solomon et al. (2007) report a warming of 2.4°C with a likely range of 2.4°C (following from the interval (1.4°C, 3.8°C)), versus a likely range of 2.7°C in our case, and for scenario A1FI they report a warming of 4.0°C with a likely range of 4.2°C (following from the interval (2.4°C, 6.4°C)), versus a likely range of 3.5°C in our case. Thus, the degree of uncertainty in our projections is comparable to Solomon et al. (2007). The IPCC presents indirectly validated multi-model outcomes, whereas our outcomes can be seen as a *direct* outcome based on statistical confidence sets, given our statistical model. This suggests that from our statistical perspective sufficient uncertainty is incorporated in the IPCC scenarios. In this sense, our results validate the IPCC outcomes.

However, we find higher temperature projections than the IPCC, although the results are not directly comparable, because Solomon et al. (2007) report the forecasted temperature change during the ten years 2090–2099 relative to 1980–1999, while we report the end-of-period (that is, in the year 2100) temperature relative to the pre-industrialization temperature level. But even when we correct for these differences, our projected temperature levels remain substantially higher. Perhaps the reason is that our simple statistical model is too simple, by ignoring important forces, such as self-regulatory mechanisms in the climate system, which are incorporated into the more advanced models employed by the IPCC. On the other hand, our more alarming empirical findings are not without support. A study by Rahmstorf et al. (2007), for example, indicates that (up to 2006) an aerosol cooling smaller than expected might be a possible cause of a realized warming in the upper part of the range projected by the IPCC. In our study we do incorporate lower levels of SO2 emissions, yielding less aerosol cooling, in line with these empirical findings.

Our temperature projections are thus located on the edge of the IPCC range; they are not in conflict with the IPCC outcomes. For scenario A1T our 95%-confidence interval (for the year 2100, relative to the pre-industrialization temperature level) is given by (3.4°C, 8.1°C), and in scenario A1FI it is given by (5.5°C, 12.8°C). Thus, using 95%-confidence intervals (and correcting for the differences in reporting), there is substantial overlap with the results by Solomon et al. (2007).

8. Conclusions

In this paper a simple model of climate change was presented —simple enough to allow rigorous statistical analysis. The analysis consisted of quantifying the uncertainty associated with projections of future climate change. We introduced our model, presented the parameter estimates, and showed that our simple model describes historical climate change well. Then we used the model to generate predictions of future climate change and, most importantly, we quantified the uncertainty associated with these predictions, distinguishing between process and parameter risk.

For the scenarios considered (the SRES scenarios A1T and A1FI), our model predicts an increase in temperature above the best guess in the most recent IPCC report (Solomon et al., 2007). However, given the range of uncertainty around our projection (quantified by

95%-confidence intervals), the IPCC projections are not ruled out. We also find, in our single model, that the uncertainty range due to parameter and process uncertainty is of the same order as the uncertainty range reported in Solomon et al.'s (2007) multi-model projections, with the empirically-based parameter risk being the dominant source of risk. One application of our statistical analysis is therefore to serve as empirical validation of the multi-model approach employed by the IPCC, which only allows for an indirect validation. Another application would be to obtain a quick, first impression of climate change consequences, including the corresponding uncertainty, under alternative scenarios.

Acknowledgments

We are grateful to Reto Knutti and an anonymous Associate Editor for helpful comments and discussion.

Appendix: Emission data

We use global data on carbon dioxide emission and sulphur dioxide emission. CO2 emissions are measured in millions of metric tons of carbon, while SO2 emissions are measured in metric tons of sulfur. For CO2 emissions we use data over the years 1959–2002 from the Carbon Dioxide Information and Analysis Center (CDIAC), available at the website

http://cdiac.ornl.gov/aboutcdiac.html.

For SO2 emissions we use data over the years 1959–2000 from David Stern's website

http://www.sterndavidi.com/datasite.html.

Data over the years 2001 and 2002 are lacking. For this reason, we estimated and applied (17) twice: once using only the available data 1959–2000, and once using these data extended by assuming that our SO2 emission data in 2001 and 2002 have the same growth as the growth of the "grand total" SO2 emissions of EDGAR v4.1. Both outcomes are quite similar. In the main text we use and report the second case only. The source of the EDGAR v4.1 data is: European Commission, Joint Research Centre (JRC)/Netherlands Environmental Assessment Agency (PBL). Emission Database for Global Atmospheric Research (EDGAR), release version 4.1, with corresponding website

http://edgar.jrc.ec.europa.eu, 2010.

References

Andreae MO, Jones CD, Cox PM (2005). "Strong Present-Day Aerosol Cooling Implies a Hot Future." *Nature*, **435**, 1187–1190.

Arellano M, Bond SR (1991). "Some Tests of Specification for Panel Data: Monte Carlo Evidence and an Application To Employment Equations." *Review of Economic Studies*, **58**, 277–297.

Blundell R, Bond SR (1998). "Initial Conditions and Moment Restrictions in Dynamic Panel Data Models." *Journal of Econometrics*, **87**, 115–143.

Brohan P, Kennedy JJ, Harris I, Tett SFB, Jones PD (2006). "Uncertainty Estimates in Regional And Global Observed Temperature Changes: A New Dataset From 1850." *Journal of Geophysical Research*, **111**, D12106.

Gilgen H, Ohmura A (1999). "The Global Energy Balance Archive." *Bulletin of the American Meteorological Society*, **80**, 831–850.

Härdle W, Linton O (1994). "Applied Nonparametric Methods." In D McFadden and RF Engle (eds.), "The Handbook of Econometrics, Vol. 4," New Holland, New York, 2295–2339.

Knutti R, Hegerl GC (2008). "The Equilibrium Sensitivity of the Earth's Temperature to Radiation Changes." *National Geoscience*, **1**, 735–743.

Knutti R, Plattner GK (2012). "Comments on 'Why Hasn't Earth Warmed as Much as Expected?'." *Journal of Climate*, **25**, 2192–2199.

Magnus JR, Melenberg B, Muris C (2011). "Global Warming and Local Dimming: The Statistical Evidence." *Journal of the American Statistical Association*, **106**, 452–464.

Majda A, Timofeyev I, Eijnden E (2001). "A Mathematical Framework for Stochastic Climate Models." *Communications on Pure and Applied Mathematics*, **54**, 891–974.

Meehl GA, Stocker TF, Collins WD, Friedlingstein P, Gaye AT, Gregory JM, Kitoh A, Knutti R, Murphy JM, Noda A, Raper SCB, Watterson IG, Weaver AJ, Zhao ZC (2007). "Global Climate Projections." In: S Solomon, D Qin, M Manning, Z Chen, M Marquis, KB Averyt, M Tignor, HL Miller (eds.), "Climate Change 2007: The Physical Science Basis. Contribution of Working Group I to the Fourth Assessment Report of the Intergovernmental Panel on Climate Change," Cambridge University Press, Cambridge, UK.

Mitchell TD, Jones PD (2005). "An Improved Method of Constructing a Database of Monthly Climate Observations and Associated High-Resolution Grids." *International Journal of Climatology*, **25**, 693–712.

Nakicenovic N, Swart R (eds.) (2000). *Emissions Scenarios*. Cambridge University Press, Cambridge, UK.

Padilla LE, Vallis GK, Rowley CW (2011). "Probabilistic Estimates of Transient Climate Sensitivity Subject to Uncertainty in Forcing and Natural Variability." *Journal of Climate*, **24**, 5521–5537.

Rahmstorf S, Cazenave A, Church JA, Hansen JE, Keeling RF, Parker DE, Somerville RCJ (2007). "Recent Climate Observations Compared to Projections." *Science*, **316**, 709.

Roe GH, Baker MB (2007). "Why is Climate Sensitivity So Unpredictable?" *Science*, **318**, 629–632.

Schwartz SE, Charlson RJ, Kahn RA, Ogren JA, Rodhe H (2010). "Why Hasn't Earth Warmed as Much as Expected?" *Journal of Climate*, **23**, 2453–2464.

Solomon S, Qin D, Manning M, Chen Z, Marquis M, Averyt KB, Tignor M, Miller HL (eds.) (2007). *Contribution of Working Group I to the Fourth Assessment Report of the Intergovernmental Panel on Climate Change*. Cambridge University Press, Cambridge, UK.

Stainforth DA, Aina T, Christensen C, Collins M, Faull N, Frame DJ, Kettleborough JA, Knight S, Martin A, Murphy JM, Piani C, Sexton D, Smith LA, Spicer RA, Thorpe AJ, Allen MR (2005). "UncertainTy in Predictions of the Climate Response to Rising Levels of Greenhouse Gases," *Nature*, **433**, 403–406.

Stern DI (2006). "Reversal of the Trend in Global Anthropogenic Sulfur Emissions." *Global Environmental Change*, **16**, 207–220.

Tselioudis G, Rossow WB (1994). "Global, Multiyear Variations of Optical Thickness with Temperature in Low and Cirrus Clouds." *Geophysical Research Letters*, **21**, 2211–2214.

Vallis GK, Gerber EP, Kushner PJ, Cash BA (2004). "A Mechanism and Simple Dynamical Model of the North Atlantic Oscillation and Annular Modes." *Journal of the Atmospheric Sciences*, **61**, 264–280.

Wild M. (2009). "GlobAl Dimming and Brightening: A Review." *Journal of Geophysical Research*, **114**, D00D16.

Wild M, Grieser J, Schär C (2008). "Combined Surface Solar Brightening and Increasing Greenhouse Effect Support Recent Intensification of the Global Land-Based Hydrological Cycle." *Geophysical Research Letters*, **35**, L17706.

Wild M, Ohmura A, Gilgen H, Rosenfeld D (2004). "On the Consistency of Trends in Radiation and Temperature Records and Implications for the Global Hydrological Cycle." *Geophysical Research Letters*, **31**, L11201.

Affiliation:

Jan R. Magnus
Department of Econometrics and Operations Research
Vrije Universiteit Amsterdam
De Boelelaan 1105
1081 HV Amsterdam, The Netherlands
Email: jan@janmagnus.nl

Bertrand Melenberg
Department of Econometrics and Operations Research
Tilburg University
PO Box 90153
5000 LE Tilburg, The Netherlands
E-mail: b.melenberg@uvt.nl

Chris Muris
Department of Economics
Simon Fraser University
8888 University Drive
Burnaby, BC V5A 1S6, Canada
Email: cmuris@sfu.ca

Martin Wild
ETH Zürich
Institute for Atmospheric and Climate Science
CHN L 16.2
Universitätstrasse 16
8092 Zürich, Switzerland
Email: martin.wild@env.ethz.ch

Journal of Environmental Statistics
Volume 5, Issue 4
August 2013

http://www.jenvstat.org
Submitted: 2013-01-10
Accepted: 2013-07-10